A Study of Combined K–π Separation Using Time of Flight Counters and a Gas Čerenkov Detector

THE HALL D DETECTOR AT JEFFERSON LAB

Curtis A. Meyer
and
Paul Eugenio

May 7, 1999

1 Introduction

This note is a follow up to note 14 [1] which examined the effects of timing resolution on K–π separation. This note extends the previous study by including a Gas Černkov counter at the down stream end of the magnet. The purpose of this note is to study the effects of the Čerenkov on the combined particle identification. In particular, we want to understand the effects of:

- the index of refraction of the gas,
- the inner radius of the detector.
- the number of sectors in the detector.

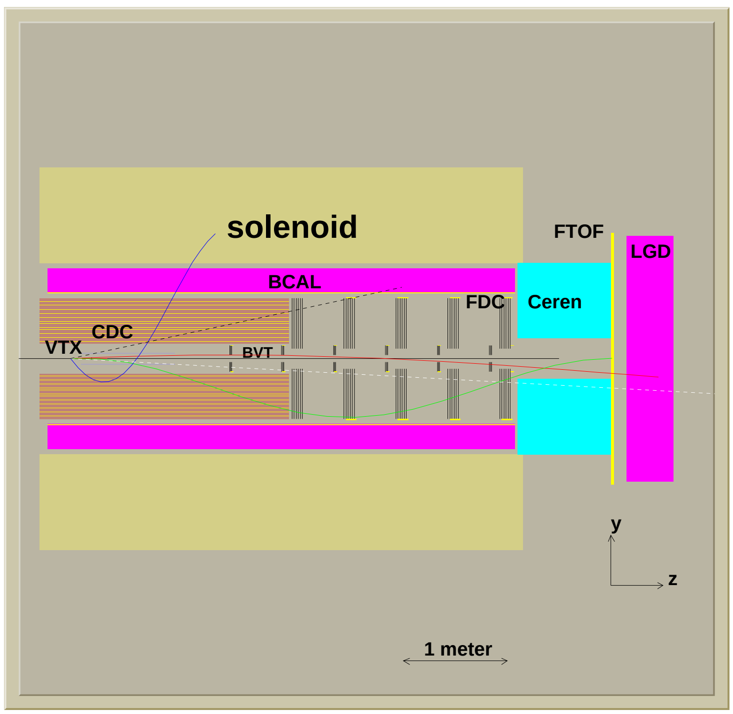

Figure 1: The Hall D Stage I detector. The central time–of–flight system is at the inside surface of the BCAL, while the forward time–of–flight system is labeled at FTOF. The event shown has both charged particles and photons in it.

2 The Forward Čerenkov System

In this study, we have assumed a time–of–flight resolution of 100 ps, (1σ). The nominal detector configuration is shown in Fig. 1. The Čerenkov detector is assumed to start at 460 cm from the upstream end of the magnet, and end at 550 cm from the upstream end. The detector is assumed to be *ring* shaped, with both the inner and outer radii as tunable parameters. In addition, the nominal index of refraction is set at $n = 1.0014$ corresponding to $\beta_{\text{threshold}} = 0.9986$. The detector nominally turns on for π's at $p_\pi = 2.64\,\text{GeV/c}$ and for K's at $p_K = 9.35\,\text{GeV/c}$. The index of refraction is also a tunable parameter.

The Monte Carlo simulation of the Černekov detector is done following the description on page 155 of the *Particle Data Book* [2]. Using the geometry of the detector, the path length, L, of the particle through the active volume is computed. Using this, and the photon energy, the mean number of collected photoelectrons is generated as in equation 1.

$$N_{\text{p.e.}} \approx L(90\,\text{cm}^{-1}) < \sin^2\theta_c > \tag{1}$$

This assumes a 90% light collection efficiency and a photocathode efficiency of 28%. The Čerenkov angle θ_c is given in equation 2.

$$\cos\theta_c = \frac{1}{\beta n} \tag{2}$$

The mean number of photoelectrons is then taken as the mean, μ, for a Poisson distribution as in equation 3, which gives the probability of observing r photoelectrons from a distribution of mean μ.

$$f(r;\mu) = \frac{\mu^r e^{-\mu}}{r!} \tag{3}$$

Each of these r photoelectrons has a second tunable detection efficiency applied to it, and this yields a number of *detected* photoelectrons. The Čerenkov counter is said to have fired if there is at least one detected photoelectron.

This study has been performed using reaction 4 with a 10 GeV photon

$$\gamma p \to K^+K^-\pi^+\pi^-p \tag{4}$$

beam. The figure of merit has been the the fraction of π's, K's and p's that have been identified as kaons. This identification is done via two criteria. The first uses the time of flight and the reconstructed momentum to compute the *mass* of the particle. Fig. 2 shows this mass as a function of time resolution in the forward system. Using this mass, we define a window around the K mass as given in equations 5, 6 and 7.

$$0.40\,\text{GeV/c}^2 < m < 0.60\,\text{GeV/c}^2 \tag{5}$$
$$0.35\,\text{GeV/c}^2 < m < 0.65\,\text{GeV/c}^2 \tag{6}$$
$$0.30\,\text{GeV/c}^2 < m < 0.70\,\text{GeV/c}^2 \tag{7}$$

In addition, we have identified all tracks that have at least one detected photoelectron in the Čerenkov system as a pion. Fig. 3 shows plots of the fraction of K's, π's and p's identified as kaons in the forward system as a function of particle's momentum. All plots assume a 100 ns time resolution. The three figures on the left use only the mass windows, while those on the right couple both the time of flight and the Čerenkov system. The assumed index of refraction of the gas in these plots is $n = 1.0014$.

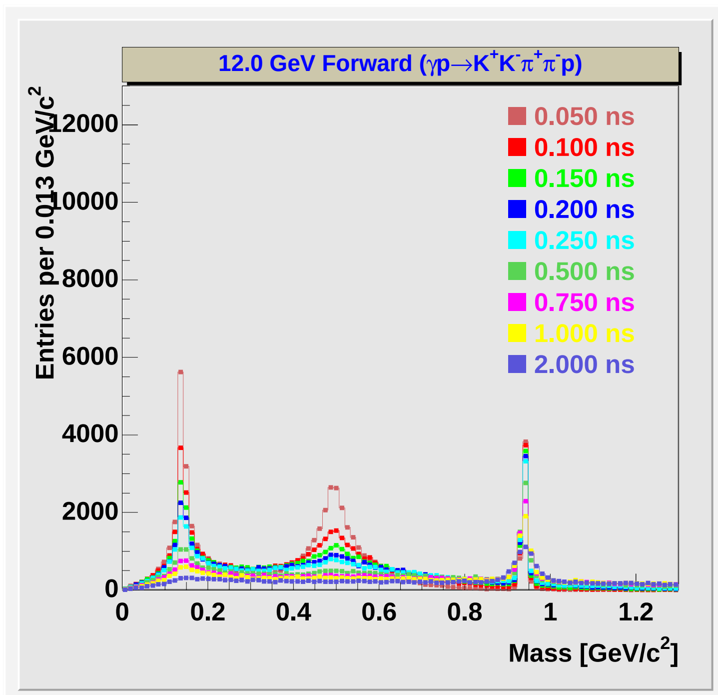

Figure 2: The reconstructed mass as a function of timing resolution in the forward region. The reaction is for $\gamma p \to K^+K^-\pi^+\pi^-p$ for a 10.0 GeV photon beam energy.

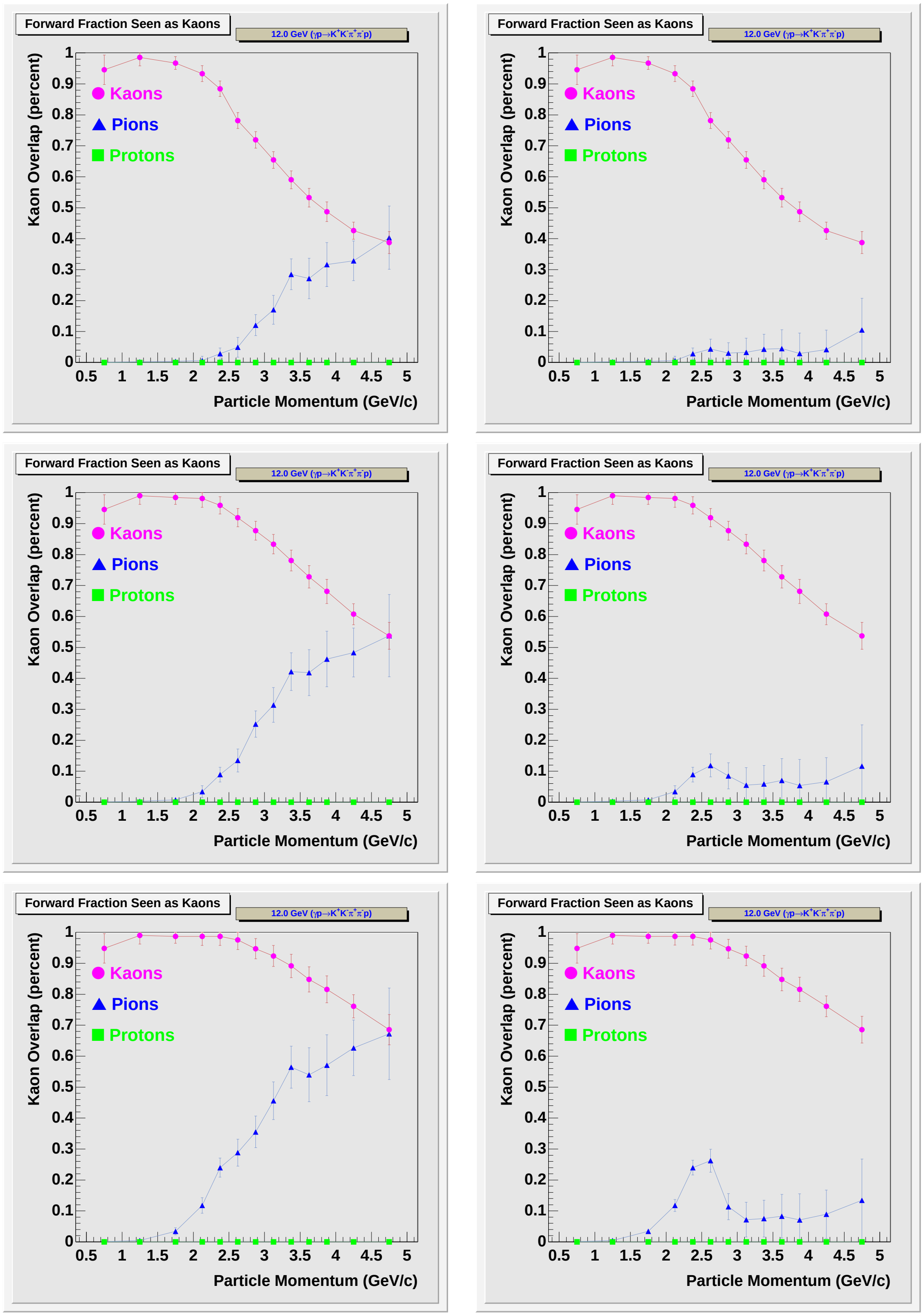

Figure 3: The fraction π's, K's and p's identified as K's as a function of the particle momentum. The three rows correspond to mass windows 5, 6 and 7 and 100 ns time resolution. The figures on the left only use time of flight, while those on the left use both time of flight, and the Černekov system.

3 The Index of Refraction

The index of refraction, n, is a property of the gas. The nominal value of $n = 1.0014$ is probably difficult to change with currently available gas mixtures. However, it is worth examining the exact effect that this gas mixture has on the K–π separation. From Fig. 4, it is clear that $n = 1.0014$

n	β	p_π	p_K
1.0010	0.9990	3.12 GeV/c	11.11 GeV/c
1.0014	0.9986	2.64 GeV/c	9.34 GeV/c
1.0024	0.9976	2.01 GeV/c	7.17 GeV/c
1.0044	0.9956	1.49 GeV/c	5.29 GeV/c

Table 1: The threshold momenta for kaons and pions as a function of the four indices of refraction given used in Fig. 4.

is not the optimum index of refraction. An index of about $n = 1.0024$ would limit feed through from π's to under 1% for most momenta up to 5 GeV/c. However, as the index starts to go above $n = 1.0024$, the K's begin to reach the Černekov threshold.

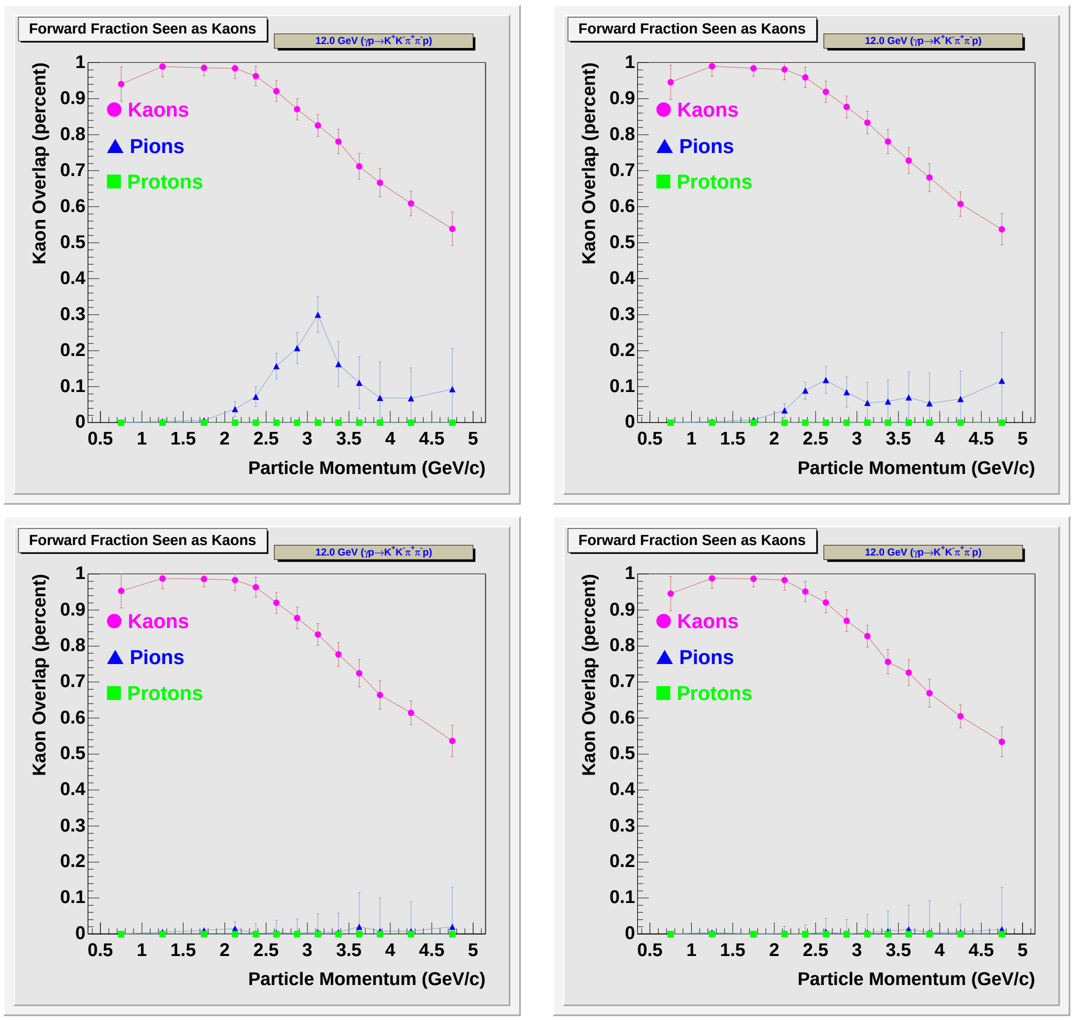

Figure 4: The fraction of K's, π's and p's which are identified as K's as a function of particle momentum. The plots use mass window 6 and the Čerenkov system. The figures going from left to right and top to bottom have $n = 1.0010$, $n = 1.0014$, $n = 1.0024$ and $n = 1.0044$.

4 The Geometry of The Detector

In terms of the Čerenkov geometry, we have concentrated on the inner and outer radii of the system. The nominal values were taken at $r_i = 20.0\,\mathrm{cm}$ and $r_o = 95.0\,\mathrm{cm}$. In figure 5 we have examined the effect that the inner radius has. The figures go from $r_i = 0.0\,\mathrm{cm}$ up to $r_i = 40\,\mathrm{cm}$. These figures indicate that at least for this particular channel, the critical inner radius is somewhere between 10 cm and 20 cm. It is probably true that for a lower multiplicity event, the optimum would be at a smaller radius. In Fig. 6, we have plotted the acceptance as a function of the outer radius of the Čerenkov counter. At least for this particular channel, the inefficiency for pions starts to degrade at about 65 cm, or at the outer radius of charged tracking in the solenoid region.

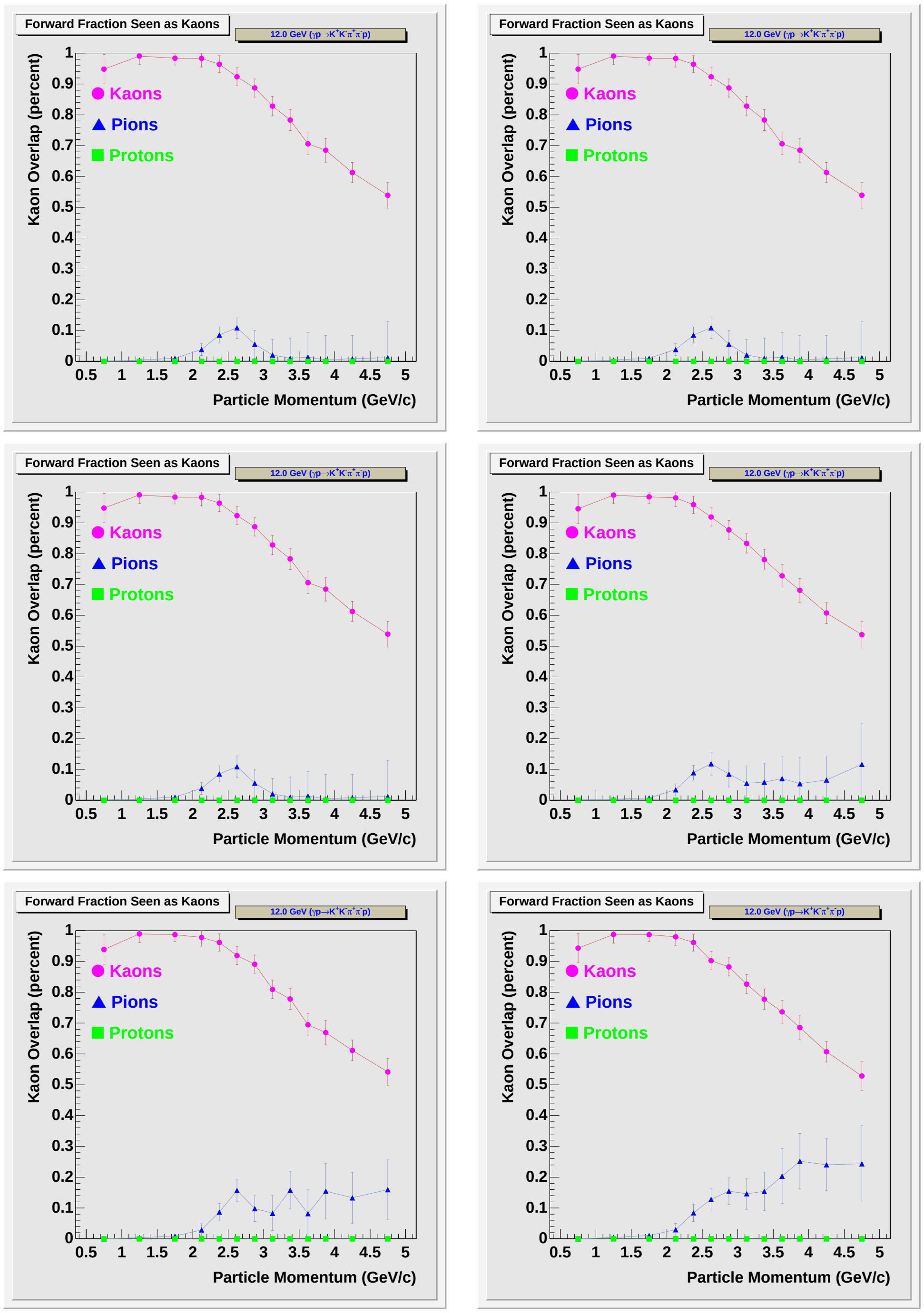

Figure 5: The fraction of K's, π's and p's which are identified as K's as a function of particle momentum. The plots use mass window 6 and the Čerenkov system with $n = 1.0014$. The figures going left to right and top to bottom are for a different inner radius of the Čerenkov system. $r = 0\,\text{cm}$, $r = 5\,\text{cm}$, $r = 10\,\text{cm}$, $r = 20\,\text{cm}$, $r = 30\,\text{cm}$ and $r = 40\,\text{cm}$.

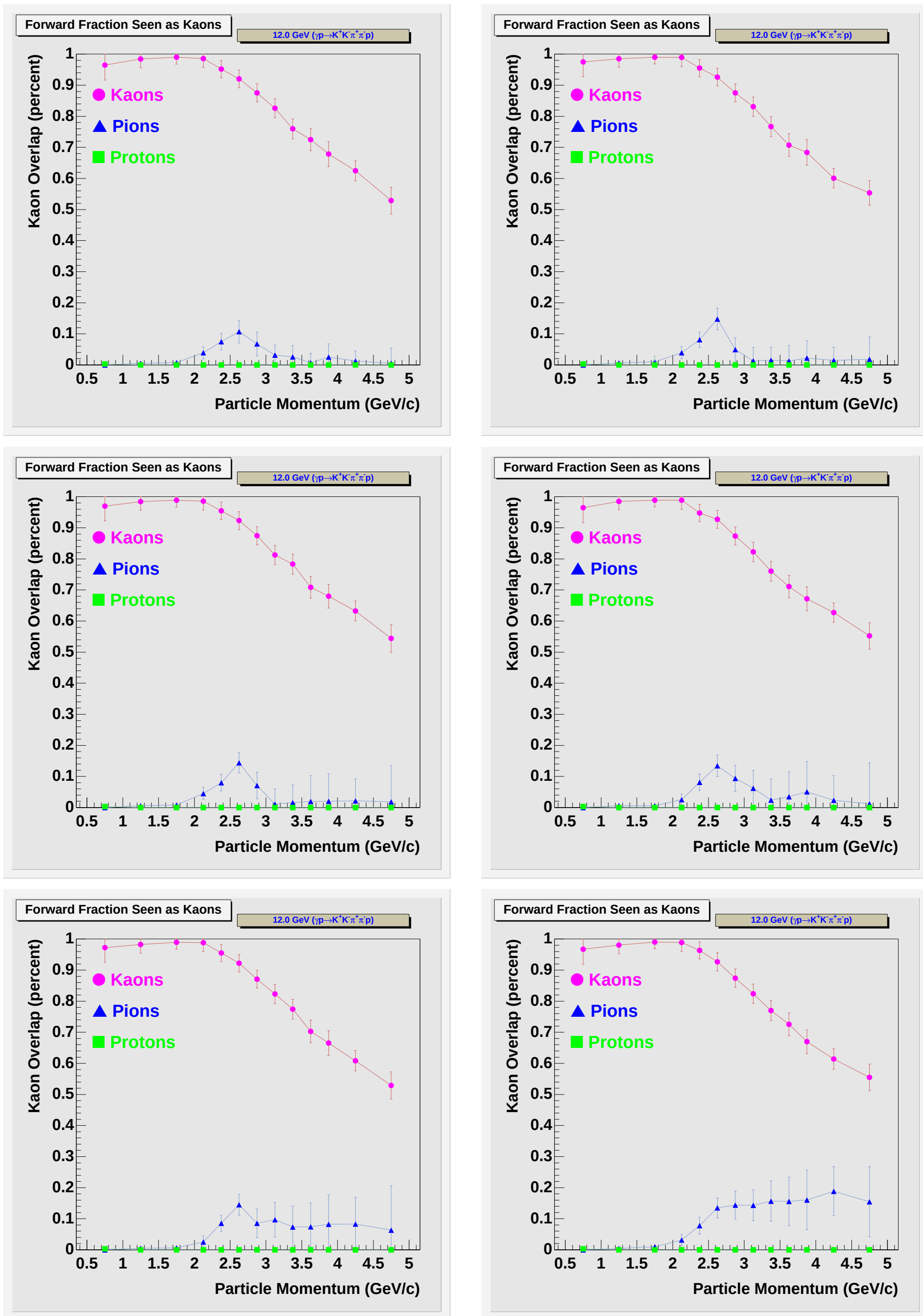

Figure 6: The fraction of K's, π's and p's which are identified as K's as a function of particle momentum. The plots use mass window 6 and the Čerenkov system with $n = 1.0014$. The figures going left to right and top to bottom are for a different outer radius of the Čerenkov system. $r = 150\,\mathrm{cm}$, $r = 95\,\mathrm{cm}$, $r = 75\,\mathrm{cm}$, $r = 65\,\mathrm{cm}$, $r = 55\,\mathrm{cm}$ and $r = 45\,\mathrm{cm}$.

5 The Segmentation of the Čerenkov

In this section, we have examined the effect of axial segmentation on the particle identification. We have assumed that if more than one particle enters a segment of the Čerenkov system, and if any of these are above the threshold for pions, it will not be possible to distinguish the response of the two. If neither particle fires, then we will be able to identify them. Table 2 summarizes the results for segmentation of 1 and 6 for two different values of n. For the nominal value of $n = 1.0014$, the segmentation does not seem to be so important. However, it is also true that things will become worse for a higher multiplicty final state.

n	*Segmentation*	*Vetoed* π's	*Vetoed* K's
1.0014	1	215/34727	261/38574
1.0014	6	39/34727	14/38574
1.0024	1	1586/34727	1742/38574
1.0024	6	296/34727	58/38574

Table 2: Segmentation Efficiencies

6 Summary and Conclusions

In this study, we have examined the combined Čerenkov and time of flight system for particle identification in the forward region of the HALL D detector system. These studies are based on the the particular channel

$$\gamma p \rightarrow K^+K^-\pi^+\pi^-p,$$

with $E_\gamma = 10\,\mathrm{GeV}$. We find that there are two parameters which most influence the efficiency of this ssytem. The inner radius of the Čerenkov system should be between 10 cm and 15 cm, and the index n should be somewhat larger than the current design value of $n = 1.0014$. An optimum would be at about $n = 1.0024$. This latter criteria may be difficult to obtain given the finite choices of gasses.

References

[1] Curtis A. Meyer, **A Study of Timing Resolutions on Particle Identification in the Hall D Detector at Jefferson Lab**, Hall D Note number 14, March 1999, (http://www.phys.cmu.edu/halld/notes_main.html).

[2] C. Caso, *et al.*, (The Particle Data Group), Eur. Phys. J. C3, 1, (1998).

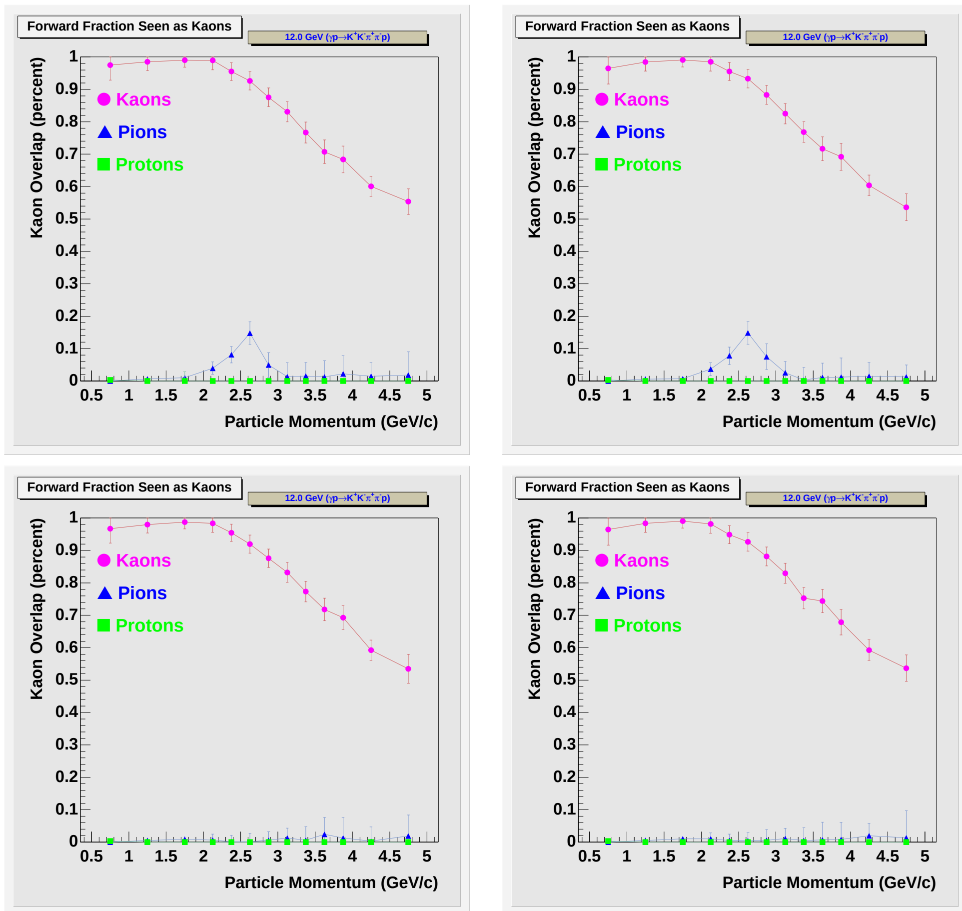

Figure 7: The fraction of K's, π's and p's which are identified as K's as a function of particle momentum. The plots use mass window 6 and the Čerenkov system with $n = 1.0014$. The upper left figure has no segmentation and $n = 1.0014$. The upper right figure has six segments with $n = 1.0014$. The upper right figure has one segment with $n = 1.0024$. The upper right figure has six segments with $n = 1.0024$.